

Generalizable Federated Learning using Client Adaptive Focal Modulation

Tajamul Ashraf

*Department of Computer Vision
MBZUAI
Abu Dhabi, Masdar City, UAE*

TAJAMUL.ASHRAF@MBZUAI.AC.AE

Iqra Altaf Gillani

*Gaash lab, Department of Information Technology
NIT Srinagar
Srinagar, Kashmir, India*

IQRAALTAF@NITSRI.AC.IN

Abstract

Federated learning (FL) has proven essential for privacy-preserving, collaborative training across distributed clients. Our prior work, TransFed, introduced a robust transformer-based FL framework that leverages a learn-to-adapt hypernetwork to generate personalized focal modulation layers per client, outperforming traditional methods in non-IID and cross-domain settings. In this extended version, we propose **AdaptFED**, where we deepen the investigation of focal modulation in generalizable FL by incorporating: (1) a refined adaptation strategy that integrates task-aware client embeddings to personalize modulation dynamics further, (2) enhanced theoretical bounds on adaptation performance, and (3) broader empirical validation across additional modalities, including time-series and multilingual data. We also introduce an efficient variant of TransFed that reduces server-client communication overhead via low-rank hypernetwork conditioning, enabling scalable deployment in resource-constrained environments. Extensive experiments on eight diverse datasets reaffirm the superiority of our method over state-of-the-art baselines, particularly in source-free and cross-task federated setups. Our findings not only extend the capabilities of focal modulation in FL but also pave the way for more adaptive, scalable, and generalizable transformer-based federated systems. The code is available at <http://github.com/Tajamul21/TransFed>

Keywords: Federated Learning, Domain Adaptation, Focal Modulation, Transformers.

1 Introduction

Federated Learning. Federated Learning (FL) is a prominent collaborative machine learning approach designed to utilize data from multiple clients without compromising their privacy Kaissis et al. (2020), Hsu et al. (2020), Zhang et al. (2021a), Tran et al. (2019). FL is a widely used iterative learning method that maximizes the value of the data acquired across multiple clients McMahan et al. (2017), Li et al. (2023b), Li et al. (2023c).

However, traditional FL methods, which aim to develop a single global model, often underperform due to the diverse data distributions and varying needs of different clients Li et al. (2020), Zhang et al. (2021b). In real-world scenarios, where datasets are **Non-IID** (not independent and identically distributed), the significant differences across data can cause the global model to deviate substantially from local data patterns Hsieh et al. (2020). This mismatch can lead to slow convergence and poor inference performance, as the global model

struggles to accommodate the unique characteristics of each client’s data. Consequently, training a single global model proves to be ineffective when dealing with heterogeneous data and system variations across different clients Zhao et al. (2018).

To deal with this challenge, personalized federated learning (pFL) mechanisms have been introduced that enable each client to train a model customized to their unique data distribution Fallah et al. (2020), Hanzely et al. (2020), Huang et al. (2021), Li et al. (2021a). Recently, pFL has gained significant attention for its ability to effectively manage statistical heterogeneity and enhance personalization in FL Tan et al. (2022), T Dinh et al. (2020), Zhang et al. (2023b), Zhang et al. (2023a). This approach represents an evolution of traditional federated learning, focusing on developing individualized models for each client.

By moving away from the single global model strategy, pFL maintains the advantages of collaborative training while better accommodating the diverse needs of different clients Sattler et al. (2019), Sattler et al. (2020). An ideal pFL system aims to achieve two main goals: aggregating information for collaborative learning and training reasonable personalized models. However, existing pFL methods often prioritize one goal over the other, leading to imbalances. Strategies such as data-based approaches, single-model techniques like regularization Li et al. (2021a), T Dinh et al. (2020) and meta-learning Fallah et al. (2020), and multiple-model approaches like decoupling model parameters Collins et al. (2021), Li et al. (2021b), Liang et al. (2020) have been proposed in the literature to address these challenges. Applying distance metrics to overall model parameters or loss values may not fully exploit client heterogeneity, hindering further

personalization and impacting pFL training efficiency. However, some pFL frameworks heavily rely on Convolutional Neural Networks (CNNs), which can be sensitive to variations in diverse data Geirhos et al. (2018). On the other hand, transformer models Vaswani et al. (2017) have shown exceptional performances in language and vision tasks. Transformers utilize a self-attention mechanism that enables them to capture global interactions among inputs. This self-attention mechanism makes transformers more resilient to distribution shifts and data heterogeneity Ramachandran et al. (2019). Recognizing the varying utilities of different transformers is crucial for improving the effectiveness of pFL methods.

Transformers in Federated Learning. Inspired by the success of self-attention mechanisms, recent research has investigated employing transformers Vaswani et al. (2017) as the core network architecture for federated learning, in conjunction with the foundational federated averaging (FedAvg) algorithm McMahan et al. (2017). While transformers have become the standard architecture in centralized computer vision tasks, their exploration in

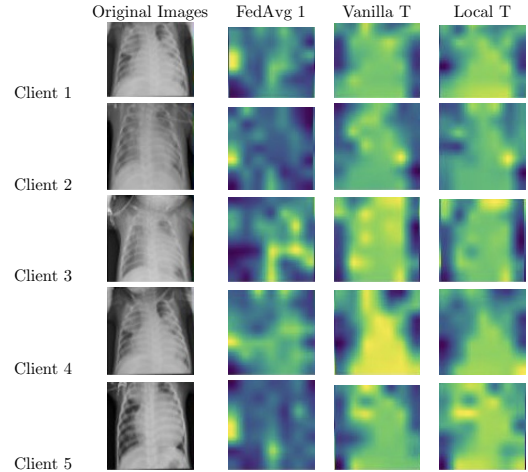


Figure 1: Comparing focal maps of Local-T, FedAvg-T, and Vanilla-T across clients, we see local training and Vanilla-T emphasize task details, while FedAvg-T disrupts such information.

federated learning (FL) remains limited. Qu et al. (2022) demonstrated the robustness of vision transformers against data heterogeneity in global FL settings. In contrast, Sun et al. (2023) and Li et al. (2023a) explored their personalization in pFL. Further research has also focused on pre-trained transformers Chen et al. (2022), Nguyen et al. (2022), Sun et al. (2023). More recently, focal modulation networks Yang et al. (2022), which replace self-attention with a new focal modulation technique to model input-dependent long-range interactions, have shown promising initial results. However, the impact of FL algorithms on focal modulation requires further investigation, as it may limit the effectiveness of FocalNet-based transformers in downstream tasks. Recent studies have underscored the pivotal role of focal modulated layers in transformers Yang et al. (2022), Wang et al. (2023), Zou et al. (2023), highlighting their superiority over other architectures. Given the potential of focal-modulated federated learning, we believe it is crucial to explore the challenges in this area comprehensively.

Main Challenges in Federated Learning. Building on this insight, we investigated focal modulation’s impact on federated learning first. Our experiments included: 1) **Local-T**, training individual Vision Transformer (ViT) models on each client; 2) **FedAvg Transformer (FedAvg-T)**, using FedAvg to train a global FocalNet model; and 3) **Vanilla Tailored-T**, maintaining local focal modulation with for server-side parameter aggregation. We extend our prior investigation by conducting experiments on the **RSNA** pneumonia dataset Wang et al. (2017), a widely used medical imaging benchmark comprising chest X-rays labeled for pneumonia. The data was partitioned across five clients to simulate heterogeneous clinical environments and client-specific variation. However, as the number of clients increases, so does the communication burden between the clients and the central server, revealing a critical bottleneck in traditional federated settings. To better understand model behavior, we generated attention maps using the Attention Rollout method Abnar and Zuidema (2020). As shown in Figure 1, both **Local-T** and **Vanilla Tailored-T** models effectively highlighted diagnostically relevant regions (yellow heatmaps), whereas the baseline **FedAvg-T** model failed to yield meaningful focal modulation attention Yang et al. (2022). This underscores the limitations of directly applying focal modulation in federated environments.

Moreover, our extended analysis confirms that focal modulation layers lack scalability, as their number grows linearly with client count. Tailoring such layers for new clients requires complete retraining, which is computationally expensive and impractical for real-world deployment. To address these limitations, **AdaptFED** builds upon our earlier work TransFed Ashraf et al. (2024), a federated transformer framework that introduced a learn-to-tailor strategy for scalable client personalization. Rather than relying on conventional FocalNet-style local adaptation, TransFed utilizes a centralized learnable generator that dynamically produces client-specific focal modulation. In this extended version, we further explore and enhance the scalability and generalization capabilities of this approach across challenging cross-domain and source-free FL settings, demonstrating its effectiveness in overcoming key limitations of focal modulation in federated environments.

Domain Adaptation in Federated Setting. In federated learning, assuming labeled data on client devices is impractical due to high costs and manual effort Yao et al. (2022). To address this, we focus on a practical scenario called Federated Source-Free Domain Adaptation (**Fed-SFDA**). Here, the model is pre-trained using the server on labeled source data but cannot access it later, following the Source-Free Domain Adaptation (SFDA) set-

ting Liu et al. (2021b). Clients can only access their unlabeled target datasets, which they cannot share, reflecting real-world conditions with limited client data. After pre-training, the process transitions to a fully unsupervised approach. **Fed-SFDA** aims to handle multi-target domain adaptation while addressing federated learning challenges like heterogeneity, communication bottlenecks, and client privacy. To our knowledge, previous works have not concurrently addressed this problem and its related issues. Our approach, **TransFED**, introduces a learnable generator on the server for matrix projections in focal modulation layers. These matrices enable adaptive queries, keys, and values, as well as parameter aggregation and sharing. By using the learn-to-tailor mechanism, **TransFED** efficiently distributes parameters and creates customized focal modulation layers. It achieves high accuracy, scalability with client numbers, and strong adaptability to new clients, making it a robust solution for **Fed-SFDA** scenarios. The primary contributions of this work are summarized as follows:

- We propose a refined *task-aware adaptation strategy* that encodes client-specific context into the hypernetwork, enabling more fine-grained personalization and improved generalization across diverse domains.
- To further push the boundaries of personalization in FL, we introduce **AdaptFED** a lightweight, communication-efficient variant of **TransFED**, which leverages low-rank conditioning in the hypernetwork to scale across clients with limited bandwidth.
- We expand the evaluation of **TransFED** to a broader range of tasks, including *multilingual language modeling*, *time-series forecasting*, and *multi-modal vision-language tasks*, demonstrating consistent improvements under severe domain shift and limited supervision.
- We revisit and extend the **Fed-SFDA** setup, Federated Source-Free Domain Adaptation, by incorporating a learnable distribution-aware generator that handles unlabeled, non-iid client data in cross-domain FL setups without access to source data.
- Our theoretical analysis offers tighter adaptation bounds for the learn-to-adapt strategy, shedding light on how hypernetwork-driven modulation achieves robust personalization in non-IID federated learning.

2 Related Work

Personalized Federated Learning (pFL). In recent years, numerous approaches have been developed to tackle heterogeneity in personalized federated learning (pFL). These methods generally fall into two broad categories: data-based and model-based strategies. Data-based approaches aim to mitigate statistical heterogeneity by modifying client datasets, while model-based methods focus on adapting model architectures or parameters to suit individual clients Zhang et al. (2022a,c). To address challenges related to data heterogeneity and privacy in pFL, researchers have proposed a range of techniques Fallah et al. (2020); Mansour et al. (2020); Wang et al. (2019). Data-based strategies often involve augmenting local datasets with a small shared global dataset or implementing client selection mechanisms to ensure a more homogeneous data distribution Zhang et al. (2022a,b,c). Model-based approaches can be further classified into single-model and multiple-model frameworks.

Single-model methods extend conventional federated learning (FL) techniques by incorporating local fine-tuning, regularization, meta-learning, model mixtures, or parameter decomposition Fallah et al. (2020); Mansour et al. (2020); Wang et al. (2019). In contrast, multiple-model approaches train several global models tailored for heterogeneous clients or facilitate collaboration to personalize models at an individual level Li et al. (2020, 2021a); T Dinh et al. (2020). Several techniques enhance personalization by fine-tuning global models on local client datasets, introducing proximal regularization, leveraging knowledge distillation, or using clustering methods to group similar clients Arivazhagan et al. (2019); Dosovitskiy et al. (2020); Mendieta et al. (2022); Sattler et al. (2020); Zhu et al. (2021). Fine-tuning the global model for each client is a common strategy for obtaining personalized parameters Fallah et al. (2020); Mansour et al. (2020); Wang et al. (2019). Proximal regularization, as implemented in methods like **FedPROX** Li et al. (2020), **pFedME** T Dinh et al. (2020), and **DITTO** Li et al. (2021a), helps mitigate client drift by constraining updates during training. **FedALIGN** Mendieta et al. (2022) tackles data heterogeneity from a generalization perspective, ensuring models remain robust across diverse client distributions.

Hybrid approaches have also emerged, such as **KNNPer** Marfoq et al. (2022), which integrates k-nearest neighbors with existing FL models to enhance personalization while preserving local feature representations. Knowledge distillation techniques like **FedMD** Li and Wang (2019) and **FedGEN** Zhu et al. (2021) use global teacher models to guide the training of client-specific models. Clustered FL methods, including **CFL** Sattler et al. (2020), **PFA** Liu et al. (2021a), and **FedAMP** Huang et al. (2021), leverage client similarities to train models more effectively within homogeneous subgroups. More recently, transformer-based approaches have been explored for federated personalization. **FedTP** Li et al. (2023a) focuses on adapting attention maps in vision transformers (ViT) Dosovitskiy et al. (2020) by decoupling cross-attention mechanisms to manage data heterogeneity. Another method, **FedREP** Arivazhagan et al. (2019), improves personalization by training local classifier heads while maintaining shared base layers across clients. Overall, these advancements highlight the growing sophistication of federated learning in addressing client heterogeneity, paving the way for more adaptive and efficient decentralized learning systems.

Federated-based Domain Adaptation Vision tasks often require dense annotations, but recent methods use synthetic data from virtual environments to reduce costs Alberti et al. (2020); Richter et al. (2016); Testolina et al. (2023); Toldo et al. (2020). However, models trained on synthetic data struggle to generalize due to domain shifts. Domain adaptation (DA) aims to bridge the gap between source and target domains, particularly in Unsupervised Domain Adaptation (UDA) scenarios where target data lacks labels. Early DA methods focused on reducing domain divergence Long et al. (2015); Saito et al. (2018), with adversarial training becoming popular involving networks and domain discriminators Luo et al. (2019); Tsai et al. (2018). Non-trainable style translation algorithms like **FDA** Yang and Soatto (2020) have been introduced to address these challenges. Modern approaches Hoyer et al. (2022); Lian et al. (2019); Zou et al. (2018) use self-learning to generate pseudo-labels from target data, enabling fine-tuning in federated settings where clients only have access to unlabeled data.

Our proposed **TransFED** framework employs a learn-to-customize mechanism to train tailored focal-modulation layers within a transformer, effectively addressing client data heterogeneity.

Unlike traditional methods, **TransFED** uses a server-based trainable generator to produce projection parameters within focal-modulation layers, enabling client-specific queries, keys, and values. This approach builds on transformer advancements in vision tasks Dosovitskiy et al. (2020) and leverages findings that transformers perform better than CNNs in heterogeneous federated learning Qu et al. (2022). **TransFED** distinguishes itself by integrating a learnable generator within a transformer, contrasting with CNN-focused methods like **pFedHN** Ha et al. (2016), **pFedLA** Ma et al. (2022), and **FedROD** Chen and Chao (2021). The study of Domain Adaptation (DA) in Federated Learning (FL), including Unsupervised Domain Adaptation (UDA) and especially Source-Free Domain Adaptation (SFDA), is still emerging. Additionally, Clustered FL (CFL) approaches group clients with similar characteristics, such as geographic location, to create personalized models for specific conditions Kundu et al. (2021), Fallah et al. (2020), Ghosh et al. (2020). Unlike these methods, we use the adaptive learnable generator to bridge cross-domain shifts.

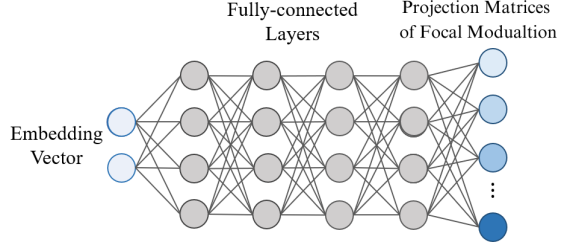


Figure 2: Structure of Hypernetwork

3 Federated Learning by Tailored Focal Modulation

This section introduces **AdaptFED**, which is specifically designed to address heterogeneity in a source-free setting and produces personalized, high-quality adaptive models for individual clients.

3.1 Problem Statement

In the context of visual tasks, the earlier **TransFED** Ashraf et al. (2024) framework incorporates the utilization of a traditional DINO model Caron et al. (2021). The initial step in processing the input sequence S , which has a fixed length l , involves partitioning the images into a sequential format during the image preprocessing phase of the **FocalNet**. Subsequently, this sequential representation is converted into an embedding matrix M , with dimensions $\mathbb{R}^{n \times m}$. The focal-modulation mechanism operates on the queries, keys, and values, denoted as $Q = MP^Q$, $K = MP^K$, and $V = MP^V$, respectively. We concatenate these projection parameters into $P = [P^Q, P^K, P^V]$ for simplicity.

By utilizing a visual feature map $X \in \mathbb{R}^{H \times P \times C}$ as the input, a standard encoding process produces a feature representation $y_i \in \mathbb{R}^C$ for each visual token (query) $Q_i \in \mathbb{R}^C$. This generation is accomplished through the token’s interaction with its surroundings, including neighboring tokens, and the aggregation of information across contexts. The process involves the interaction function τ and the aggregation function A . Consequently, the refined representation y_i is obtained by combining the aggregated context features, obtained through the function A at each location i , with the query Q_i through the interaction function τ . Focal Modulation generates refined representation y_i using an early aggregation procedure formulated as:

$$y_i = \tau(A(i, X), Q_i) \quad (1)$$

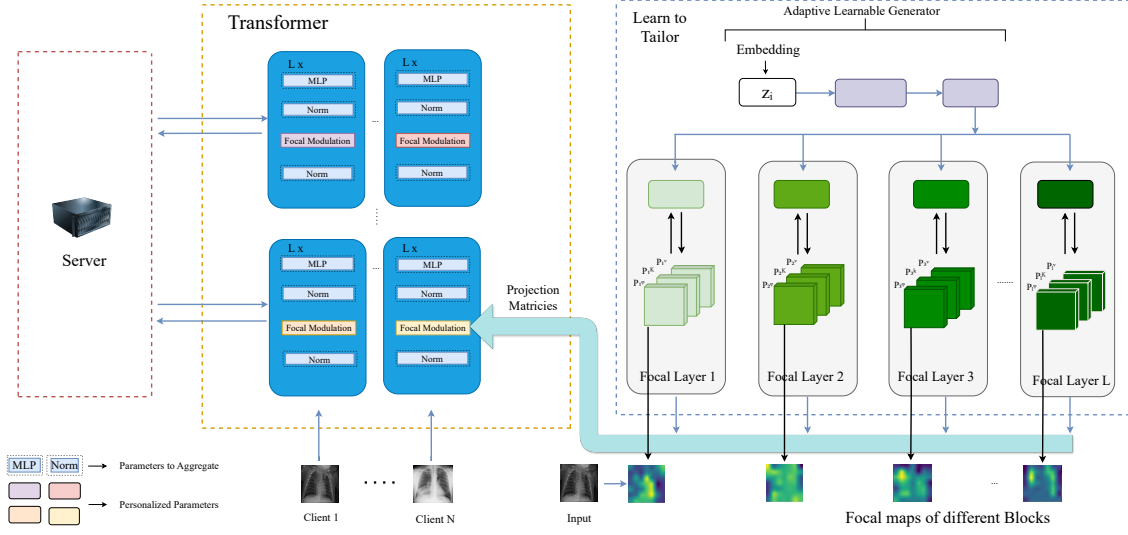


Figure 3: **AdaptFED Overview:** The architecture combines focal modulation layers and centralized parameter aggregation to enhance collaborative learning while preserving personalization. Clients retain self-attention layers locally, while a server-based hypernetwork generates personalized projection matrices, ensuring adaptation to diverse data distributions.

where the context features are first aggregated using A at each location i , then the query interacts with the aggregated feature based on τ to form y_i . To emulate a federated scenario, we examine a collection of N clients designated by $[N]$, with each specific client i holding its own local dataset $D_i = (x_i^{(j)}, y_i^{(j)})_{j=1}^{m_i}$ ($1 \leq i \leq N$), consisting of m_i samples drawn from a distinct data distribution P_i . The total dataset is denoted as $D = \bigcup_{i \in [N]} D_i$, with a total size of $S = \sum_{i=1}^N m_i$. The customized model associated with client i , defined by the parameters θ_i , is denoted as $f(\theta_i; \cdot)$. The optimization objective is defined as follows:

$$\arg \min_{\Theta} \sum_{i=1}^N \left(\frac{m_i}{S} \right) K_i(\theta_i) \quad (2)$$

where $K_i(\theta_i) = \mathbb{E}_{(x_i^{(j)}, y_i^{(j)}) \in D_i} [l(f(\theta_i; x_i^{(j)}), y_i^{(j)})]$. Here, $\Theta = \theta_{i=1}^N$ represents the set of tailored parameters for each client, and $l(\cdot, \cdot)$ denotes the per-sample loss function that is common to all clients. The selection of the loss function for a specific task, whether it is a mean square error or cross-entropy loss, is contingent upon the nature of the task.

3.2 Vanilla Tailoring of Focal Modulation

Federated learning's popularity stems from global insights via focal modulation layers. However using **AdaptFED** on client layers can harm performance with diverse data. To address this challenge, our solution involves tailored focal modulation. This approach entails customizing certain local layers while averaging other layers to maintain standard insights.

Algorithm 1 TransFed: Generalizable Focal Modulation

Require: C (rounds), L (local epochs), α (local LR), β (global LR).

- 1: Initialize parameters ξ^0 , z_i^0 for all clients i , and ϕ^0
- 2: **for** $c = 1$ to C **do**
- 3: Sample client set $C_c \subset \{1, \dots, N\}$
- 4: **for** $i \in C_c$ **do**
- 5: $\xi_i^{c,0} \leftarrow \bar{\xi}^{c-1}$ \triangleright broadcasted init for client i
- 6: $P_i^{c,0} \leftarrow h(\phi^{c-1}, z_i^{c-1})$
- 7: $\theta_i^{c,0} \leftarrow \{P_i^{c,0}, \xi_i^{c,0}\}$
- 8: **for** $k = 0$ to $L - 1$ **do**
- 9: Sample mini-batch $B_i \subset D_i$
- 10: $\theta_i^{c,k+1} \leftarrow \theta_i^{c,k} - \alpha \nabla_{\theta_i} \mathcal{L}_i(\theta_i^{c,k}; B_i)$
- 11: **end for**
- 12: $\Delta P_i \leftarrow P_i^{c,L} - P_i^{c,0}$
- 13: **end for**
- 14: $\bar{\xi}^c \leftarrow \sum_{i \in C_c} \frac{m_i}{\sum_{j \in C_c} m_j} \xi_i^{c,L}$
- 15: $\phi^c \leftarrow \phi^{c-1} - \beta \sum_{i \in C_c} \frac{m_i}{\sum_{j \in C_c} m_j} \nabla_{\phi} P_i^c \Delta P_i$ \triangleright global meta-params
- 16: **for** $i \in C_c$ **do**
- 17: $z_i^c \leftarrow z_i^{c-1} - \beta \nabla_{z_i} P_i^c \Delta P_i$ \triangleright client-specific aux update (no sum over i)
- 18: **end for**
- 19: **end for**
- 20: **return** $\bar{\xi}^C$, ϕ^C , $\{z_i^C\}_{i=1}^N$

In **AdaptFED**, parameters are locally trained and aggregated on the server, similar to **FedAvg**. The focal-modulation layer has projection parameters P_i , while other layers have parameters ξ . The tailored model, denoted as $\theta_i = (P_i, \xi)$, undergoes local training. This process is repeated for multiple communication rounds. Resulting in the updated model $f(P_i^{t,k}, \bar{\xi}_i^{t,k}; \cdot)$, where $P_i^{t,k}$ is retained locally to store the tailored information of client i , and $\bar{\xi}_i^{t,k}$ is aggregated across the clients using Equation (2):

$$\bar{\xi}^t = \sum_{i=1}^N \left(\frac{m_i}{S} \right) \xi_i^{t,k} \quad (3)$$

Consequently, the objective function of **AdaptFED**, as derived from Equation (1), is to minimize the following loss:

$$\arg \min_{\theta} \sum_{i=1}^N \left(\frac{m_i}{S} \right) K_i(P_i, \xi) \quad (4)$$

where

$$K_i(P_i, \xi) = \sum_{i=1}^N \left(\frac{m_i}{M} \right) \mathbb{E}_{(x_i^j, y_i^j) \in D_i} l(f(P_i, \xi; x_i^{(j)}), y_i^{(j)}) \quad (5)$$

While the vanilla customization procedure generates tailored focal-modulation layers through local training, it overlooks the potential inherent client relationships, leading to sub-

optimal tailored models. Moreover, the scalability of tailored focal-modulation layers becomes an issue as the number of clients grows linearly. Additionally, the adaptation capability of tailored Focal Modulation is limited, requiring retraining when novel clients are introduced to obtain specific focal modulation layers for them.

3.3 Custom Learning for Focal Modulation

This section introduces **AdaptFED**, a framework that incorporates a learn-to-tailor approach to augment the existing vanilla customization mechanism for focal Modulation.

Algorithm 1 presents the **AdaptFED** process for parameter updates in a federated learning scenario. It spans communication rounds (C) and local epochs (L), iterating through clients to locally update model parameters (θ) using mini-batches. Global parameters ϕ and z_i are also updated collectively, yielding refined global parameters $\bar{\xi}^t$, ϕ^t , and z^t . These enhancements encourage effective collaboration among clients while retaining individual data characteristics. In the **AdaptFED** approach, an adaptive learnable generator Ha et al. (2016) is integrated into the server’s functionality, generating projection matrices intended for the focal-modulation layers of individual clients (as illustrated on the right side of Figure 3). This design facilitates the effective sharing of parameters among the clients.

The adaptive learnable generator at the server, denoted as $h(\phi; z_i)$ and parameterized by ϕ , takes as input an adaptive learnable embedding vector $z_i \in \mathbb{R}^D$ associated with client i , which can either be a client-specific embedding or a fixed vector. We implement the adaptive learnable generator using simple fully connected layers, where each transformer block’s last layer is unique. The z_i vector, the adaptive learnable generator produces the projection parameters $P_i = h(\phi; z_i)$ for client i , which are decomposed into the query, key, and value projection matrices for the focal-modulation mechanism, denoted as $P_i = [P_{Qi}, P_{Ki}, P_{Vi}]$.

This approach enables the adaptive learnable generator to learn a set of projection parameters $P_i = h(\phi; z_i) | 1 \leq i \leq N$ for tailored Focal Modulation. Consequently, the tailored model is represented as $f(P_i, \xi; \cdot) = f(h(z_i; \phi), \xi; \cdot)$, and loss function is updated as follows:

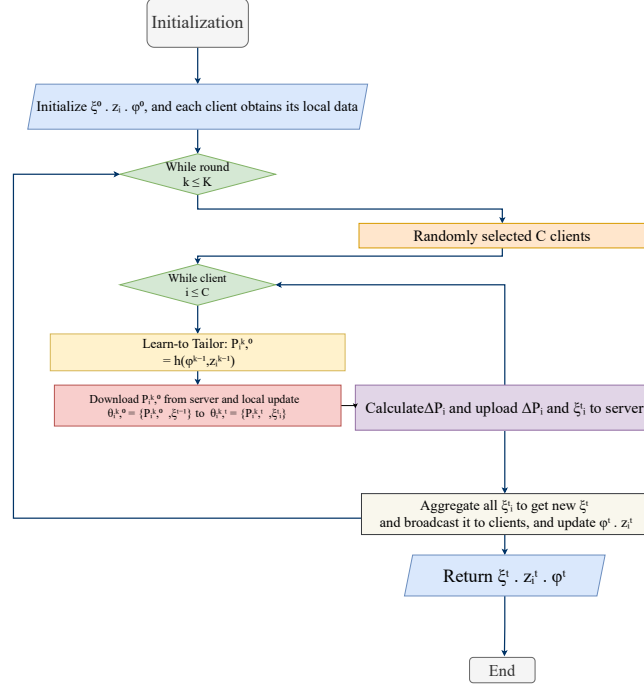


Figure 4: Visualization of Client Embeddings Learned by **AdaptFED** using t-SNE on the RSNA Dataset.

$$K_i(P_i, \xi) = K_i(h(\phi; z_i), \xi) = \sum_{i=1}^N \left(\frac{m_i}{M} \right) \mathbb{E}_{(x_i^j, y_i^j) \in D_i} l(f(h(\phi; z_i), \xi; x_i^{(j)}), y_i^{(j)}) \quad (6)$$

This updated loss function computes the training loss for client i by applying the adaptive learnable generator-generated projection parameters $P_i = h(\phi; z_i)$ alongside the standard parameters ξ to the tailored model. The update mechanism within each epoch is represented by the variable k , and the local model parameter θ_i is subjected to updates through stochastic gradient descent (SGD), as defined by the following equation:

$$\theta_i^k \leftarrow \theta_i^{k-1} - \alpha \nabla_{\theta_i} K_i(\theta_i^{k-1}; B_i) \quad (7)$$

where B_i represents a mini-batch extracted from D_i .

Representing the collection of selected clients in each round t as C_t . The gradients of ϕ and z_i can be obtained from Equation (6) using the chain rule:

$$\nabla_{\phi} K_i = \sum_{i \in C^t} \left(\frac{m_i}{M} \right) \nabla_{\phi} P_i^{\top} \Delta_{P_i} \quad (8)$$

$$\nabla_{z_i} K_i = \sum_{i \in C^t} \left(\frac{m_i}{M} \right) \nabla_{z_i} P_i^{\top} \Delta_{P_i} \quad (9)$$

where $\Delta P_i = P_{Ki} - P_{Qi}$ represents the change in projection parameters after K epochs of local updates.

During communication round t , updates are applied to the adaptive learnable generator parameter ϕ and the client embedding z_i through the utilization of computed gradients:

$$\phi^t = \phi^{t-1} - \beta \nabla_{\phi} K_i^{(t-1)} \quad (10)$$

$$z_i^t = z_i^{t-1} - \beta \nabla_{z_i} K_i^{(t-1)} \quad (11)$$

Contrasted with the standard customization method, the learn-to-tailor approach within **AdaptFED** brings forth a range of benefits. Firstly, it achieves effective parameter sharing across clients while harnessing the focal modulation mechanism's potency in federated learning. Secondly, its scalability accompanies an expanding client base, owing to the shared adaptive learnable generator with personalized embedding vectors driving the focal modulation layer's generation. Lastly, its adaptability extends to new clients whose data remains unseen during training. The initial and final aspects will undergo validation in Section IV. The middle aspect is substantiated by a comparison of parameter counts between learn-to-customize and standard customization. The adaptive learnable generator, adopting an MLP architecture, comprises parameters roughly equivalent to $D_h \times D_s$, where D_h and D_s denote the dimensions of the hidden layers within the adaptive learnable generator and the self-attention projection parameters, respectively. In contrast, the cumulative self-attention projection parameters in the standard customization rise linearly with the client count, i.e., $N \times D_s$. With a substantial client count ($N > D_h$), learn-to-customize for focal modulation consumes fewer resources.

3.4 Fed-SFDA Setting

In this section, we formalize the proposed Federated Source-Free Domain Adaptation (**Fed-SFDA**) setting. We consider a central server and a set of clients K with $|K| = K$. The source dataset D_S , kept on the server, consists of image-segmentation label pairs $(x_S, y_S) \sim P_S(x, y)$, where $x_S \in X$ and $y_S \in Y^{N_p}$. Each client $k \in K$ has a target training dataset D_{T_k} with images $x_{T_k, i} \sim P_{T_k}(x)$. The source and test datasets share the same categories $Q = Q_S = Q_T$. Clients' local datasets, drawn from a meta-distribution with G latent visual domains, may have similar distributions. The test dataset $D_{T_{\text{test}}}$ follows the target distribution P_T and evaluates the final model.

The first step of **Fed-SFDA** involves pre-training on D_S . To align source and target styles, we apply FDA Yang and Soatto (2020) style transfer. Clients extract and send their style s_k to the server, which augments D_S with these styles for training. After pre-training, D_S is no longer used. Pseudo-labels help mimic label presence but can lead to overconfidence and misclassifications. To address this, we use a Knowledge Distillation (KD) loss \mathcal{L}_{KD} to retain pre-trained knowledge. However, KD alone can lead to slight overfitting. To mitigate this, we apply Stochastic Weight Averaging (SWA) to clients' teachers g_c .

$$w_{t+\omega}^{g_c} = \frac{w_t^{g_c} n_t^{g_c} + w_{t+\omega}^c}{n_t^{g_c} + 1}$$

where $n_t^{g_c} = \frac{t-t_{\text{START}}}{\omega}$. This technique, called **SWA** teacher, reduces noise and stabilizes the learning curve, enabling better convergence to the local minimum of the total loss:

$$L = L_{\text{PSEUDO}} + \lambda_{\text{KD}} L_{\text{KD}}$$

where L_{PSEUDO} is the pseudo-label loss and λ_{KD} is a hyperparameter controlling the KD loss.

3.5 Generalization Bound

We analyze the generalization bound of **AdaptFED** in this section. Before starting the analysis, we first introduce some assumptions as follows.

Assumption 1 *The embedding vectors z_i and the weights φ of the hypernetwork $h(\varphi, z_i)$ are assumed to lie within a bounded region with radius R_h . Similarly, the parameters ξ of other layers in the Transformer are constrained within a bounded region of radius R_t . Formally, these constraints can be expressed as:*

$$\|\varphi - \varphi'\| \leq R_h, \quad \|z_i - z'_i\| \leq R_h, \quad \|\xi - \xi'\| \leq R_t. \quad (12)$$

Assumption 2 (*Lipschitz Conditions*) *Let $\mathcal{D}_1, \mathcal{D}_2, \dots, \mathcal{D}_N$ denote the real data distributions. Define the expected loss as $\mathcal{LD}_i(h(\varphi; z_i), \xi) = \mathbb{E}(x, y) \in \mathcal{D}_i(l(f(h(\varphi; z_i), \xi; x), y))$. We assume that the following Lipschitz conditions are satisfied:*

$$|\mathcal{LD}_i(h(\varphi; z_i), \xi) - \mathcal{LD}_i(h(\varphi; z_i), \xi')| \leq L_\xi \|\xi - \xi'\|, \quad (13a)$$

$$\begin{aligned} & |\mathcal{LD}_i(h(\varphi; z_i), \xi) - \mathcal{LD}_i(h'(\varphi; z_i), \xi)| \\ & \leq L_h \|h(\varphi; z_i) - h'(\varphi; z_i)\|, \end{aligned} \quad (13b)$$

$$\|h(\varphi; z_i) - h(\varphi'; z_i)\| \leq L_\varphi \|\varphi - \varphi'\|, \quad (13c)$$

$$\|h(\varphi; z_i) - h(\varphi; z'_i)\| \leq L_z \|z_i - z'_i\|. \quad (13d)$$

Theorem 1 *Let $\hat{\mathcal{D}}_1, \hat{\mathcal{D}}_2, \dots, \hat{\mathcal{D}}_N$ represent the empirical data distributions for N clients. The parameters $\hat{\varphi}$, \hat{z}_i , and $\hat{\xi}$ are obtained by training on these empirical distributions. Define \mathcal{H} as the set of personalized hypotheses, and let d denote the VC-dimension of \mathcal{H} . Assuming that Assumptions 1 and 2 are satisfied, the following holds with probability at least $1 - \delta$:*

$$\left| \sum_{i=1}^N \frac{m_i}{M} \mathcal{L}_{\mathcal{D}_i}(h(\hat{\varphi}; \hat{z}_i), \hat{\xi}) - \sum_{i=1}^N \frac{m_i}{M} \mathcal{L}_{\mathcal{D}_i}(h(\varphi^*; z_i^*), \xi^*) \right| \leq \sqrt{\frac{M}{2} \log \frac{N}{\delta}} + \sqrt{\frac{dN}{M} \log \frac{eM}{d}} + L_h R_h (L_\varphi + L_z) + L_\xi R_t \quad (14)$$

where φ^* , z_i^* , and ξ^* represent the optimal parameters corresponding to the real distribution of each client, respectively; the size of the whole dataset is M with the local data size of client i being m_i .

Theorem 1 highlights that the performance of a model trained on empirical distributions is influenced by the complexity of the hypothesis class \mathcal{H} (quantified by its VC-dimension), the number of clients, the total dataset size, and the associated Lipschitz constants.

The second term on the right-hand side of (14) can be expressed as $\sqrt{\frac{\log(eM/d)}{M/dN}}$, indicating its dependency on the ratio $\frac{M}{d}$. We define the hypothesis classes of **AdaptFED** with the *learn-to-personalize* mechanism and vanilla personalization as \mathcal{H}_h and \mathcal{H}_v , respectively. The VC-dimension of \mathcal{H}_h is smaller than that of \mathcal{H}_v , particularly when the number of clients is large. This reduction arises because **AdaptFED** employs a single hypernetwork to generate self-attention layers for all clients via the *learn-to-personalize* mechanism as shown in Figure 2. As the VC-dimension d decreases, the value of $\sqrt{\frac{\log(eM/d)}{M/dN}}$ also reduces. Consequently, **AdaptFED** achieves better generalization compared to vanilla personalization for self-attention layers, especially in scenarios with a large number of clients.

The detailed key lemmas and the proof of Theorem 1 are provided in the Appendix below.

4 Experiments

This section introduces the experimental configuration, assesses our proposed model’s performance, and compares several baseline methods across diverse learning scenarios. We introduce the benchmarks, **Non-IID** settings, model architectures used in our experiments, and relevant implementation details. The performance evaluation focuses on analyzing different aspects of our model, including the impact of network backbones and customized components of the transformer, the adaptation ability to novel clients, the compatibility of **AdaptFED** with other methods, and the visualization of attention maps. Additionally, we investigate the effect of heterogeneity in label distribution, noise-induced feature imbalances, and the influence of different parameters. To provide a clear overview of the experimental framework, Figure 3 depicts the flowchart of our **AdaptFED** approach. This section outlines our model’s experimental design, performance evaluation metrics, and key

findings, providing valuable insights into its effectiveness and versatility in various learning scenarios.

4.1 Experimental Setup

Table 1: Datasets and Models.

Dataset	Task	Clients	Samples	Model
RSNA Wang et al. (2017)	Image. Classification.	100/200	30,227	FocalNet
Kermany Kermany et al. (2018)	Image. Classification.	100/200	5,232	FocalNet
Shakespeare Shakespeare. (1994)	Character. Prediction.	683	2,578,349	LSTM, Transformer
CIFAR-10 Krizhevsky et al. (2009)	Image. Classification.	100/200	60,000	FocalNet
CIFAR-100 Krizhevsky et al. (2009)	Image. Classification.	100/200	60,000	FocalNet
Office-Caltech Gong et al. (2012)	Image. Classification.	50/100	2,533	FocalNet

4.1.1 BASELINES

Our evaluation comprehensively compared the **AdaptFED** with various federated learning algorithms. We compared **AdaptFED** against fundamental federated algorithms, including **FedAvg** McMahan et al. (2017) and **FedPROX** Li et al. (2020). Additionally, we evaluated its performance against state-of-the-art (SOTA) customization algorithms, including **FedPER** Arivazhagan et al. (2019), **pFedME** T Dinh et al. (2020), and **FedTP** Li et al. (2023a), as well as Vanilla-based models. Also, we compare our method with state-of-the-art source-free domain adaptation (SFDA) methods Feng et al. (2023). By including these various algorithms in our comparison, we aimed to assess the effectiveness and superiority of **AdaptFED** in achieving customized and efficient federated learning. The selected algorithms represent a range of approaches that tackle different aspects of customization in federated learning, allowing us to evaluate **AdaptFED**’s performance with basic and advanced techniques. This comprehensive evaluation provides valuable insights into the relative strengths and weaknesses of **AdaptFED** compared to existing state-of-the-art algorithms, further highlighting its potential as an advanced customization approach in the domain of federated learning.

4.1.2 DATASETS

We conducted experiments on five different diverse datasets as shown in Table 1. Experiments were conducted on two widely used pneumonia benchmark datasets: **Kermany** Kermany et al. (2018) and **RSNA** Wang et al. (2017). Additionally, to validate our approach on other domains, we performed experiments on the publicly available datasets **CIFAR-10** Krizhevsky et al. (2009), **CIFAR-100** Krizhevsky et al. (2009), and **Shakespeare** McMahan et al. (2017). In addition to this, we compare our method within the Source-Free Domain Adaptation (SFDA) setting on **Office-Caltech** Gong et al. (2012) for image classification tasks in a federated learning (FL) setup.

We utilized two partitioning techniques to simulate non-identically distributed (Non-IID) scenarios in our experiments. These techniques were applied to four image datasets and one language dataset. For the image datasets, we employed two distinct split strategies to create Non-IID conditions. The first strategy, known as the *Pathological* setting, involved assign-

Table 2: **AdaptFED**’s average test accuracy is evaluated against multiple transformer-based approaches across diverse **Non-IID** scenarios, showcasing its robustness and effectiveness relative to other advanced methods.

# distribution # no. of clients	RSNA dataset				Kermany dataset			
	Pathological	Pathological	Beta	Beta	Pathological	Pathological	Beta	Beta
	100	200	100	200	100	200	100	200
Local-T	84.55±0.15	82.21±0.08	69.94±0.13	66.68±0.13	55.91±0.17	49.25±0.11	27.87±0.12	23.34±0.10
FedAvg-T	50.42±4.22	46.28±4.23	61.85±1.50	59.23±1.93	34.02±0.88	30.20±0.95	38.64±0.22	34.89±0.45
FedPER-T	89.86±0.89	89.01±0.12	79.41±0.16	77.70±0.14	67.23±0.32	61.72±0.16	37.19±0.18	29.58±0.14
FedTP-T	79.75±0.22	75.46±0.11	77.25±0.69	71.13±0.84	48.61±0.45	46.05±0.47	36.63±0.98	25.13±0.35
pFedHN-T	82.26±0.61	77.57±0.52	71.45±0.87	68.13±0.67	53.08±0.72	39.94±0.91	33.25±0.77	29.14±0.98
Vanilla-T	91.83±0.27	91.28±0.12	89.23±0.78	87.77±0.37	88.67±0.54	88.23±0.11	87.74±0.12	87.26±0.85
AdaptFED	92.67±0.74	91.34±0.86	88.49±0.38	88.16±0.33	89.80±0.23	87.73±0.74	87.34±0.92	86.98±0.64

ing classes to each client in a randomized manner. Specifically, for a given class c and client i , the sample rate was determined by $a_{i,c}/\sum_j a_{j,c}$, where $a_{i,c}$ is a value drawn from a uniform distribution $U(0.4, 0.6)$. The second strategy involved creating a federated version of the datasets by partitioning samples with the same labels across clients. This was achieved using a symmetric *Beta distribution* with a parameter of $\alpha = 0.3$. This approach ensured that samples were distributed among clients in a federated manner, promoting a diverse distribution of data for training. To enhance the realism of the local datasets within the **Kermany** dataset and **CIFAR-100**, we employed a two-stage Pachinko allocation method. Initially, a Beta distribution with a parameter of $\alpha = 0.4$ was generated over coarse labels for each client. In the second stage, a Beta distribution with a parameter of $\beta = 10$ was generated over the fine labels corresponding to the coarse labels. The class distribution and the allocation of classes in both the training and test sets were kept consistent for the coarse and fine label partitions among clients. Table 1 provides a summary of the datasets, their associated tasks, and the counts of clients and models involved.

For the **Shakespeare** dataset split in training and testing, we used the standard 80%-20% split, following established practices. Additionally, we utilized the **Office-Caltech** dataset, which consists of 10 common classes shared by the **Office-31** Saenko et al. (2010) and **Caltech-256** Griffin et al. (2007) datasets. This dataset encompasses four domains: Amazon (A), Webcam (W), DSLR (D), and Caltech (C).

4.1.3 ADAPTFED SETUP

Following the experimental setup described in **pFedHN**, we performed experiments using **AdaptFED** and benchmark methods with 100 and 200 clients. For the **Kermany** dataset, we considered 5% participation, while for the **RSNA** dataset, we considered 10% participation. The image classification task involved training each algorithm for 2000 communication rounds. **pFedHN** was trained for 4000 global communication rounds to ensure equivalent communication costs. For the detection task, the methods were trained for 300 communication rounds.

Both tasks used the SGD optimizer with a learning rate (lr) of 0.01 and a batch size (B) of 32. In **AdaptFED**, the Learnable generators were optimized similarly with $\beta = 0.01$.

Table 3: Evaluation of **AdaptFED** and Benchmark Methods on Image Datasets Under Various Non-IID Settings

# distribution # no. of clients	RSNA dataset				Kermanshah dataset			
	Pathological	Pathological	Beta	Beta	Pathological	Pathological	Beta	Beta
	100	200	100	200	100	200	100	200
FedAvg McMahan et al. (2017)	37.46±0.81	39.86±0.85	52.80±0.95	48.80±0.18	31.88±0.08	28.80±0.26	48.82±0.31	38.72±0.89
FedPER Arivazhagan et al. (2019)	82.46±0.91	81.56±0.17	78.71±0.08	75.61±0.43	59.08±0.77	60.34±0.11	38.08±0.44	28.41±0.78
pFedME T Dinh et al. (2020)	83.81±0.48	85.91±0.07	75.14±0.38	78.22±0.92	62.72±0.08	61.84±0.70	38.94±0.09	31.55±0.16
FedPROX Li et al. (2020)	39.87±0.64	44.50±0.90	56.73±0.25	49.06±0.24	34.71±0.46	30.84±0.34	51.66±0.83	39.28±0.77
FedBN Li et al. (2021b)	85.41±0.84	87.65±0.74	81.65±0.31	79.98±0.04	66.41±0.30	63.25±0.73	48.36±0.40	48.89±0.36
pFedHN Ha et al. (2016)	88.12±0.32	89.51±0.87	83.13±0.30	83.06±0.54	55.91±0.17	49.25±0.11	27.87±0.12	23.34±0.10
FedTP Li et al. (2023a)	87.85±0.44	88.36±0.50	85.63±0.30	80.65±0.41	68.99±0.25	69.25±0.74	51.78±0.05	48.85±0.11
pFedGP Achituve et al. (2021)	89.77±0.21	89.01±0.78	85.44±0.39	81.44±0.41	77.43±0.37	78.36±0.26	63.85±0.22	57.41±0.91
FedROD Chen and Chao (2021)	89.54±0.75	90.27±0.07	84.25±0.36	85.16±0.98	81.78±0.17	83.74±0.98	73.87±0.75	66.23±0.75
AdaptFED (Ours)	92.67±0.74	91.34±0.86	88.49±0.38	88.16±0.33	89.80±0.23	87.73±0.74	87.34±0.92	86.98±0.64

Experiments were conducted on a cluster with an NVIDIA Tesla V100 GPU, simulating both the server and clients.

4.2 Implementation Details

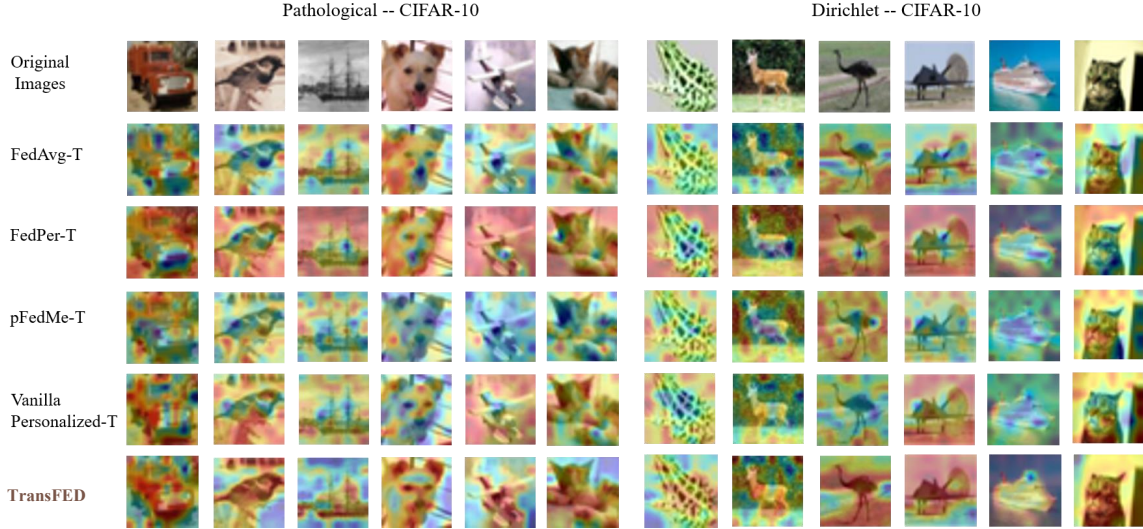
Following the experimental setup of **pFedHN** Ha et al. (2016), we implemented **FedTP** Li et al. (2023a) along with benchmark methods under standardized conditions. For the **CIFAR-10** dataset, we used 50 clients with a participation rate of 10%, while for **CIFAR-100**, we used 100 clients with a participation rate of 5%. The image classification models were trained for 1500 communication rounds, whereas **pFedHN** was trained for 5000 rounds to maintain equivalent communication costs. For the next-character prediction task, all methods were trained for 300 communication rounds. We employed the SGD optimizer across all tasks, using a learning rate of 0.01, a batch size of 64, and 5 local epochs per round. In **FedTP** and **pFedHN**, hypernetworks were optimized with SGD using $\beta = 0.01$. All experiments were conducted on a computing cluster equipped with an RTX 2080 Ti GPU, with implementations carried out in PyTorch.

4.2.1 PERFORMANCE ANALYSIS ON PNEUMONIA DATASETS

We conducted a comprehensive performance comparison between **AdaptFED** and several well-known federated learning methods, designed initially based on CNN backbones. Table 2 displays the average test accuracy of these algorithms, highlighting **AdaptFED**’s remarkable performance superiority over each of them. This result strongly supports the assertions made in our Introduction section: 1) The **FedAvg** algorithm could impede the distinctive client representations within transformer models, as evidenced by **Local-T** outperforming **FedAvg-T**; and 2) **AdaptFED**’s learned customized focal modulation effectively addresses data heterogeneity. As depicted in Table 2, **AdaptFED** consistently outperforms Vanilla customized-T across all settings, thereby confirming that the “learn-to-tailor” approach leverages the strengths of focal modulation in transformer models. To deepen our understanding, we evaluated test accuracy along with the curve depicting global communication rounds in **AdaptFED** as shown in Table 3. The analysis reveals that **AdaptFED** demonstrates a smooth curve and achieves higher accuracy compared to alternative approaches.

Table 4: Comparison of Results: **AdaptFED** and Benchmark Methods on Image Datasets with Varied Non-IID Settings.

settings Client	CIFAR 10				CIFAR 100			
	Pathological		Dirichlet		Pathological		Dirichlet	
	50	100	50	100	50	100	50	100
FedAvg McMahan et al. (2017)	47.79 \pm 4.48	44.12 \pm 3.10	56.59 \pm 0.91	57.52 \pm 1.01	15.71 \pm 0.35	14.59 \pm 0.40	18.16 \pm 0.58	20.34 \pm 1.34
FedPROX Li et al. (2020)	50.81 \pm 2.94	57.38 \pm 1.08	58.51 \pm 0.65	56.46 \pm 0.66	19.39 \pm 0.63	21.32 \pm 0.71	19.18 \pm 0.30	19.40 \pm 1.76
FedPER Arivazhagan et al. (2019)	83.39 \pm 0.47	80.99 \pm 0.71	77.99 \pm 0.02	74.21 \pm 0.07	48.32 \pm 1.46	42.08 \pm 0.18	22.60 \pm 0.59	20.06 \pm 0.26
pFedME T Dinh et al. (2020)	86.09 \pm 0.32	85.23 \pm 0.58	76.29 \pm 0.44	74.83 \pm 0.28	49.09 \pm 1.10	45.57 \pm 1.02	31.60 \pm 0.46	25.43 \pm 0.52
FedBN Li et al. (2021b)	87.45 \pm 0.95	86.71 \pm 0.56	74.63 \pm 0.60	75.41 \pm 0.37	50.01 \pm 0.59	48.37 \pm 0.56	28.81 \pm 0.50	28.70 \pm 0.46
pFedHN Ha et al. (2016)	88.38 \pm 0.29	87.97 \pm 0.70	71.79 \pm 0.57	68.36 \pm 0.86	59.48 \pm 0.67	53.24 \pm 0.31	34.05 \pm 0.41	29.87 \pm 0.69
pFedGP Achituve et al. (2021)	89.20 \pm 0.30	88.80 \pm 0.20	80.44 \pm 0.83	78.29 \pm 1.13	63.30 \pm 0.10	48.98 \pm 0.01	34.28 \pm 0.34	28.29 \pm 1.53
FedTP Li et al. (2023a)	90.31 \pm 0.26	88.39 \pm 0.14	81.24 \pm 2.17	80.27 \pm 0.28	68.05 \pm 0.24	63.76 \pm 0.39	46.35 \pm 0.29	43.74 \pm 0.39
FedROD Chen and Chao (2021)	89.87 \pm 0.03	89.05 \pm 0.04	75.01 \pm 0.09	73.99 \pm 0.09	63.30 \pm 0.10	61.30 \pm 0.20	27.04 \pm 0.73	28.29 \pm 1.53
AdaptFED (Ours)	93.47\pm0.75	91.85\pm0.39	82.89\pm0.75	79.75\pm0.15	71.96\pm0.54	68.11\pm0.39	51.75\pm0.12	44.33\pm0.74

Figure 5: Saliency maps of **AdaptFED** and other Transformer-based variants evaluated on **CIFAR-10** with 50 clients.

4.2.2 CIFAR 10 AND CIFAR 100

In our comprehensive comparative analysis of the experimental outcomes, as detailed in Table 4, our novel **AdaptFED** model emerges as a standout performer in direct contrast to the state-of-the-art benchmark methods. Across a diverse range of Non-IID settings utilizing the **CIFAR-10** and **CIFAR-100** datasets, **AdaptFED** consistently demonstrates superior accuracy rates. This distinctive performance advantage is particularly evident when considering various client populations, encompassing both 50 and 100 clients. The noteworthy enhancement **AdaptFED** brings over **FedTP** significantly emphasizes the effectiveness of our approach in managing personalized and task-specific learning objectives within the broader context of federated learning. These findings strongly validate **AdaptFED**’s ability to excel in complex scenarios characterized by heterogeneous and personalized data

Table 5: Classification accuracy (%) on the Office-Caltech dataset Griffin et al. (2007) using various federated domain adaptation (DA) methods, with baseline results reproduced from Peng et al. (2019).

Method	C,D,W→A	A,D,W→C	A,C,W→D	A,C,D→W	Avg
ResNet101 He et al. (2016)	81.9	87.9	85.7	86.9	85.6
AdaBN Li et al. (2016)	82.2	88.2	85.9	87.4	85.7
AutoDIAL Maria Carlucci et al. (2017)	83.3	87.7	85.6	87.1	85.9
f-DAN1 Long et al. (2015); Peng et al. (2019)	82.7	88.1	86.5	86.5	85.9
f-DANN2 Ganin and Lempitsky (2015); Peng et al. (2019)	83.5	88.5	85.9	87.1	86.3
FADA Peng et al. (2019)	84.2	88.7	87.1	88.1	87.1
FedRF_TCA Peng et al. (2023)	94.1	98.1	98.9	88.9	95.0
AdaptFED (Ours)	95.6	98.3	99.1	93.4	96.9

distributions, effectively positioning it as a highly promising solution for effectively addressing the inherent challenges within federated learning paradigms. Figure 5 presents a visual comparison of attention maps between FedTP and other Transformer-based variants on CIFAR-10 and CIFAR-100. Both Vanilla Personalized-T and AdaptFED exhibit client-specific self-attention, producing distinct and interpretable visualization maps. Notably, AdaptFED consistently emphasizes critical regions of test objects more effectively than PFedME and FedAvg, demonstrating its ability to capture personalized attention patterns. These results further validate AdaptFED’s effectiveness in adapting to client heterogeneity and enhancing model performance.

4.2.3 SHAKESPEARE DATASET

We compared AdaptFED with state-of-the-art federated learning methods using CNN/LSTM architectures. Table 6 summarizes their average test accuracy across image and language datasets. AdaptFED consistently outperforms baselines, highlighting its effective personalized learning and robust parameter optimization. Its efficient parameterization reduces computational overhead and enhances adaptability to heterogeneous client data, achieving superior performance over the state-of-the-art.

4.2.4 FEDERATED SOURCE-FREE DOMAIN ADAPTATION (FED-SFDA)

Table 5 presents a comprehensive evaluation of AdaptFED, showcasing its state-of-the-art (SOTA) performance against benchmark federated domain adaptation (DA) methods. Additionally, we assess the robustness of AdaptFED in the presence of message and client dropouts caused by unstable network conditions. Comparing settings (II) and (III) to setting (I) in Table 5, we observe that restricting communication to a randomly selected subset S_t of source clients and asynchronously aggregating the classifier does not degrade AdaptFED’s performance. Furthermore, AdaptFED achieves optimal results on the **Office-Caltech** dataset, further demonstrating its effectiveness and resilience in diverse federated learning scenarios.

4.2.5 ANALYSIS OF DIFFERENT ADAPTED PARTS

Table 7: The Test Accuracy Averages Across 100 Clients for Federated Transfer Learning with Pre-trained Models (**TransFED**) and Its Variants.

setting	RSNA		Kermany	
	Pathological	Beta	Pathological	Beta
TransFED (ours)	92.67 \pm 0.74	88.49 \pm 0.38	89.80 \pm 0.23	87.34 \pm 0.92
TransFED +KNN	82.34 \pm 0.43	83.65 \pm 0.52	83.79 \pm 0.24	83.95 \pm 0.37
TransFED +FedPER	88.45 \pm 0.14	86.36 \pm 0.17	87.76 \pm 0.14	85.97 \pm 0.16
TransFED +FedROD	89.56 \pm 0.45	86.55 \pm 0.27	86.23 \pm 0.37	87.22 \pm 0.39

This study examined the effects of personalizing various components of the transformer model. Specifically, we focused on four components: (1) the focal-modulation layers (our proposed method), (2) the Multi-layer perceptron layers, (3) the normalization layers, and (4) the encoder. To maintain a fair comparison, we employed the identical Learnable generator to generate the parameters associated with these individual components while ensuring consistency in the **FocalNet** structures as described. The results of this experiment are presented in Table 9. It is evident from the table that personalizing the focal-modulation layers yields the best performance compared to personalizing other components. Furthermore, Table 9 illustrates that customizing the normalization layers yields superior performance compared to tailoring the MLP layers and the absolute encoder.

Table 6: Comparative Analysis of Average Test Accuracy for Various Methods on the **Shakespeare** Language Dataset.

Method	Venue	Test Accuracy
FedAvg McMahan et al. (2017)	PMLR'17	56.86 \pm 0.86
FedPROX Li et al. (2020)	MLS'20	56.68 \pm 1.09
FedPER Arivazhagan et al. (2019)	Arxiv'19	68.71 \pm 0.65
pFedME T Dinh et al. (2020)	NeurIPS'20	63.14 \pm 1.12
MIME SGD Karimireddy et al. (2020a)	ICML'21	56.26 \pm 0.25
MIME SGDM Karimireddy et al. (2020a)	ICML'21	54.00 \pm 1.28
MIMELite Karimireddy et al. (2020a)	ICML'21	52.48 \pm 1.12
FedCM Xu et al. (2021)	IJCNN'21	38.90 \pm 1.12
SCAFFOLD Karimireddy et al. (2020b)	PMLR'20	56.68 \pm 1.66
FedDyn Acar et al. (2021)	ICLR'21	54.54 \pm 0.64
AdaBest Varno et al. (2022)	ECCV'22	58.12 \pm 0.18
FedACG Kim et al. (2024)	CVPR'24	56.79 \pm 1.25
AdaptFED (Ours)		87.57 \pm 0.47

4.2.6 GENERALIZATION TO NOVEL CLIENTS

We thoroughly assessed our method's capacity for generalization, contrasting it with **pFedME**, **pFedHN**, **FedROD**, and a customized-T Vanilla approach on the **Kermany** and **RSNA** datasets under the Beta configuration. To simulate a realistic scenario, 30% of the clients were randomly selected as novel clients whose data had not been seen during the training phase. **FedPER** fine-tuned the customized parameters in the last classification layer, while **pFedME** learned all parameters to obtain customized models for each client. In the case of **pFedHN** and **AdaptFED**, the customized parameters had the option to choose between clients embedding vectors with a dimension of 32 and the entire Learnable generator. As presented in Table 8, the outcomes suggest that **AdaptFED** (Adaptive Learnable generator) exhibits improved resilience and adeptly adjusts to new clients in a few epochs.

Table 8: Generalization Performance Comparison on **RSNA** dataset.

Method	Personalization	Client Acc (%)	Epochs
pFedME T Dinh et al. (2020)	All Parameters	78.3	8
FedTP Li et al. (2023a)	Self Attention Layers	81.2	4
pFedHN (Embedding) Ha et al. (2016)	Clientwise Embedding	79.5	6
pFedHN (Hypernetwork) Ha et al. (2016)	Whole Hypernetwork	80.2	5
FedROD Chen and Chao (2021)	Last Classification Layer	77.8	10
Vanilla Personalized-T	SA Projection Matrices	76.7	12
AdaptFED (Learnable Generator)	Focal Modulation Layers	82.6	3

4.2.7 ANALYSIS OF ADAPTIVE LEARNABLE GENERATORS

To thoroughly examine the impact of adaptive Learnable generators, we conducted a comparative analysis between **AdaptFED** and Vanilla customized-T. The latter method restores the projection parameters P_i for each client locally, without the utilization of Learnable generators. As depicted in Table 2, **AdaptFED** exhibits a significant advantage over Vanilla customized-T, highlighting the crucial role of Learnable generators in **AdaptFED**. We also observed that even when Learnable generators solely generate the parameters of the focal-modulation layer, they effectively encode client-specific information into client embeddings z_i . The Learnable generators can project client embeddings z_i onto a manifold defined by the parameters ϕ of the Learnable generator.

To delve deeper into the acquired client embeddings, we utilized the **t-SNE** algorithm for their projection onto a 2-D plane, as illustrated in Figure 6. Specifically, we distributed each coarse class among five clients, ensuring that the corresponding fine classes were uniformly allocated among these selected clients. We also trained **AdaptFED** and visualized the client embeddings after training. Learned individual embeddings of clients who share common coarse labels tend to cluster together, while those with dissimilar coarse labels are mapped farther apart. This outcome provides compelling evidence supporting our claim that Learnable generators are highly effective for encoding customized information into client embeddings z_i .

4.3 Ablation Study

4.3.1 EXTENSION

In this section, we investigate the compatibility of **AdaptFED** with existing methods that utilize personalized classifier heads such as **FedPER** Arivazhagan et al. (2019), **FedROD** Chen and Chao (2021), and methods employing local memory like **KNNPer** Marfoq et al. (2022). These modules were integrated into **AdaptFED** and evaluated on the **CIFAR-10/CIFAR-100** datasets. For **AdaptFED +FedPER**, each client retains its classification head locally within the **AdaptFED** framework. **AdaptFED +FedROD** combines the output of the personalized classification head and the global classification head to compute prediction logits. **AdaptFED +KNNPer** establishes and maintains a local repository akin to **KNNPer**, utilizing the **FAISS** library Johnson et al. (2019). Table 7 presents the results of these experiments.

Table 9: Average test accuracy of models with varying customized components.

Customized Part	RSNA		Kermany	
	Pathological	Beta	Pathological	Beta
Focal Modulation	92.67 \pm 0.74	88.49 \pm 0.38	89.80 \pm 0.23	87.34 \pm 0.92
MLP Layers	88.45 \pm 0.14	86.36 \pm 0.17	87.76 \pm 0.14	85.97 \pm 0.16
Normalization Layers	89.56 \pm 0.45	86.55 \pm 0.27	86.23 \pm 0.37	87.22 \pm 0.39
Encoder	82.34 \pm 0.43	83.65 \pm 0.52	83.79 \pm 0.24	83.95 \pm 0.37

4.3.2 EFFECT OF HETEROGENEITY IN LABEL DISTRIBUTION:

Data heterogeneity, particularly in label distribution, presents a significant challenge in personalized federated learning. To analyze its impact, we conducted experiments on the **RSNA** and **Kermany** datasets while varying the Beta distribution parameter α . Our results demonstrate that **AdaptFED** consistently outperforms state-of-the-art (SOTA) methods. In previous experiments, we examined label distribution heterogeneity by sampling class distributions from a Dirichlet distribution with $\alpha = 0.3$. To extend this analysis, we now consider a broader range of cases with $\alpha = \{0.1, 0.3, 0.5, 0.7, 0.9\}$ on the **CIFAR-10** and **CIFAR-100** datasets, where smaller α values indicate higher data heterogeneity.

Using **FedAvg-T** as a baseline, we compared **AdaptFED** against personalized federated learning methods, including **FedPER-T**, **pFedHN**, and **FedBN**. As shown in Table 10, **FedAvg-T** exhibits decreasing performance as data heterogeneity increases, while methods incorporating personalized modules demonstrate improved robustness. Among these approaches, **AdaptFED** consistently achieves the best performance across all levels of data heterogeneity, highlighting its ability to effectively mitigate challenges posed by non-IID label distributions. As α increases, certain personalized federated learning methods struggle to fully exploit client heterogeneity, occasionally performing worse than **FedAvg-T** in accuracy. However, **AdaptFED** maintains

strong and stable performance, underscoring its capability to leverage client-specific data distributions effectively, even when heterogeneity is less pronounced. Furthermore, we evaluated **AdaptFED**'s resilience under increasing levels of Gaussian noise added to client data. Consistently, **AdaptFED** outperformed competing methods, demonstrating superior robustness in handling client-specific noise. Additionally, we examined the effect of varying the number of focal modulation blocks in **AdaptFED**. Our results, summarized in Table 4, indicate that increasing the number of modulation blocks enhances the model's ability to capture data heterogeneity and improves overall performance. Based on these findings, we set the default number of focal modulation blocks to eight in subsequent experiments. Finally, we investigated the impact of different client participation rates on model per-

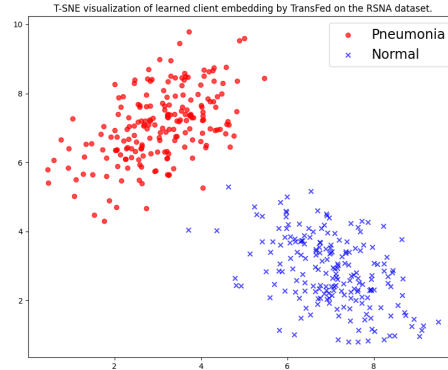


Figure 6: Visualization of client embeddings learned by **AdaptFED** using t-SNE on the **RSNA** dataset.

Table 10: Results of TransFED and Benchmark Methods on Image Datasets Over 100 Clients with Different α of Dirichlet Setting. Red color denotes second highest.

α	RSNA Test Accuracy (%)			Kermany Test Accuracy (%)		
	0.1	0.5	0.9	0.1	0.5	0.9
FedAvg-T McMahan et al. (2017)	40.99 \pm 1.25	39.23 \pm 0.63	33.57 \pm 0.58	45.29 \pm 1.54	31.82 \pm 0.42	29.14 \pm 0.81
FedPER-T Arivazhagan et al. (2019)	77.45 \pm 0.14	64.57 \pm 0.14	62.44 \pm 0.22	60.11 \pm 0.21	51.13 \pm 0.14	35.92 \pm 0.23
pFedHN Ha et al. (2016)	73.16 \pm 1.80	70.47 \pm 0.38	65.42 \pm 0.15	51.61 \pm 0.04	47.62 \pm 0.75	36.45 \pm 0.50
FedTP Li et al. (2023a)	79.67 \pm 1.42	71.36 \pm 0.86	63.74 \pm 0.19	58.19 \pm 0.81	49.86 \pm 0.05	37.37 \pm 0.95
FedBN Li et al. (2021b)	84.93 \pm 0.53	62.41 \pm 0.37	51.79 \pm 0.35	65.57 \pm 0.12	52.70 \pm 0.47	44.10 \pm 0.84
TransFED (Ours)	90.41 \pm 0.30	85.28 \pm 0.91	73.75 \pm 0.26	68.16 \pm 0.88	62.12 \pm 0.73	51.09 \pm 0.26

formance. Compared to FedAvg-T, AdaptFED exhibited greater stability across varying participation levels, reinforcing its robustness in federated learning settings with dynamic client availability.

5 Conclusion and Future Work

We presented AdaptFED, a scalable and adaptable extension of TransFED that learns to personalize focal modulation layers via a centralized, learn-to-adapt hypernetwork. By conditioning on task-aware client embeddings, AdaptFED tailors modulation dynamics to heterogeneous data distributions. We further provided enhanced theoretical guarantees with tighter adaptation/generalization bounds, and validated the approach across diverse modalities: including vision, time series, and multilingual text, demonstrating consistent improvements over FedAvg and strong personalized FL baselines, as well as over our original TransFED, in both source-free and cross-task federated settings. In addition, a low-rank hypernetwork conditioning variant reduces server-client communication overhead, enabling deployment in resource-constrained environments without sacrificing accuracy.

Future Work. Looking ahead, we plan to (i) study privacy-preserving embedding construction and auditing, (ii) integrate quantized/sparse hypernetwork updates for further efficiency, (iii) extend to continual and cross-task adaptation at larger scales, and (iv) tighten theory for non-convex transformers under realistic FL heterogeneity. We hope AdaptFED and our codebase will facilitate more adaptive, scalable, and generalizable transformer-based federated systems.

5.1 Data Availability

We do not generate any datasets, because our work proceeds within a theoretical and mathematical approach. All data used for the experiments are publically available benchmark datasets. The code and model are released publicly.

References

- S. Abnar and W. Zuidema. Quantifying attention flow in transformers. *arXiv preprint arXiv:2005.00928*, 2020.

- D. A. E. Acar, Y. Zhao, R. M. Navarro, M. Mattina, P. N. Whatmough, and V. Saligrama. Federated learning based on dynamic regularization. *arXiv preprint arXiv:2111.04263*, 2021.
- I. Achituve, A. Shamsian, A. Navon, G. Chechik, and E. Fetaya. Personalized federated learning with gaussian processes. *Advances in NeurIPS*, 34:8392–8406, 2021.
- E. Alberti, A. Tavera, C. Masone, and B. Caputo. Idda: A large-scale multi-domain dataset for autonomous driving. *IEEE Robotics and Automation Letters*, 5(4):5526–5533, 2020.
- M. G. Arivazhagan, V. Aggarwal, A. K. Singh, and S. Choudhary. Federated learning with personalization layers. *arXiv preprint arXiv:1912.00818*, 2019.
- T. Ashraf, F. Bin Afzal Mir, and I. A. Gillani. Transfed: A way to epitomize focal modulation using transformer-based federated learning. In *Proceedings of the IEEE/CVF Winter Conference on Applications of Computer Vision*, pages 554–563, 2024.
- M. Caron, H. Touvron, I. Misra, H. Jégou, J. Mairal, P. Bojanowski, and A. Joulin. Emerging properties in self-supervised vision transformers. In *Proceedings of the IEEE/CVF ICCV*, pages 9650–9660, 2021.
- H.-Y. Chen and W.-L. Chao. On bridging generic and personalized federated learning for image classification. *arXiv preprint arXiv:2107.00778*, 2021.
- H.-Y. Chen, C.-H. Tu, Z. Li, H.-W. Shen, and W.-L. Chao. On the importance and applicability of pre-training for federated learning. *arXiv preprint arXiv:2206.11488*, 2022.
- L. Collins, H. Hassani, A. Mokhtari, and S. Shakkottai. Exploiting shared representations for personalized federated learning. In *ICML*, pages 2089–2099. PMLR, 2021.
- A. Dosovitskiy, L. Beyer, A. Kolesnikov, D. Weissenborn, X. Zhai, T. Unterthiner, M. Dehghani, M. Minderer, G. Heigold, S. Gelly, et al. An image is worth 16x16 words: Transformers for image recognition at scale. *arXiv preprint arXiv:2010.11929*, 2020.
- A. Fallah, A. Mokhtari, and A. Ozdaglar. Personalized federated learning with theoretical guarantees: A model-agnostic meta-learning approach. *Advances in NeurIPS*, 33:3557–3568, 2020.
- Z. Feng, Y. Wang, J. Li, F. Yang, J. Lou, T. Mi, R. Qiu, Z. Liao, et al. Robust and communication-efficient federated domain adaptation via random features. *arXiv preprint arXiv:2311.04686*, 2023.
- Y. Ganin and V. Lempitsky. Unsupervised domain adaptation by backpropagation. In *ICML*, pages 1180–1189. PMLR, 2015.
- R. Geirhos, P. Rubisch, C. Michaelis, M. Bethge, F. A. Wichmann, and W. Brendel. Imagenet-trained cnns are biased towards texture; increasing shape bias improves accuracy and robustness. *arXiv preprint arXiv:1811.12231*, 2018.
- A. Ghosh, J. Chung, D. Yin, and K. Ramchandran. An efficient framework for clustered federated learning. *Advances in NeurIPS*, 33:19586–19597, 2020.

- B. Gong, Y. Shi, F. Sha, and K. Grauman. Geodesic flow kernel for unsupervised domain adaptation. In *2012 IEEE CVPR*. IEEE, 2012.
- G. Griffin, A. Holub, and P. Perona. Caltech-256 object category dataset. 2007.
- D. Ha, A. Dai, and Q. V. Le. Hypernetworks. *arXiv preprint arXiv:1609.09106*, 2016.
- F. Hanzely, S. Hanzely, S. Horváth, and P. Richtárik. Lower bounds and optimal algorithms for personalized federated learning. *Advances in NeurIPS*, 33:2304–2315, 2020.
- K. He, X. Zhang, S. Ren, and J. Sun. Deep residual learning for image recognition. In *Proceedings of the IEEE CVPR*, pages 770–778, 2016.
- L. Hoyer, D. Dai, and L. Van Gool. Daformer: Improving network architectures and training strategies for domain-adaptive semantic segmentation. In *Proceedings of the IEEE/CVF CVPR*, 2022.
- K. Hsieh, A. Phanishayee, O. Mutlu, and P. Gibbons. The non-iid data quagmire of decentralized machine learning. In *ICML*. PMLR, 2020.
- T.-M. H. Hsu, H. Qi, and M. Brown. Federated visual classification with real-world data distribution. In *Computer Vision–ECCV 2020: 16th European Conference, Glasgow, UK, August 23–28, 2020, Proceedings, Part X 16*, pages 76–92. Springer, 2020.
- Y. Huang, L. Chu, Z. Zhou, L. Wang, J. Liu, J. Pei, and Y. Zhang. Personalized cross-silo federated learning on non-iid data. In *Proceedings of the AAAI Conference on Artificial Intelligence*, volume 35, 2021.
- J. Johnson, M. Douze, and H. Jégou. Billion-scale similarity search with gpus. *IEEE Transactions on Big Data*, 7(3), 2019.
- G. A. Kaissis, M. R. Makowski, D. Rückert, and R. F. Braren. Secure, privacy-preserving and federated machine learning in medical imaging. *Nature Machine Intelligence*, 2(6): 305–311, 2020.
- S. P. Karimireddy, M. Jaggi, S. Kale, M. Mohri, S. J. Reddi, S. U. Stich, and A. T. Suresh. Mime: Mimicking centralized stochastic algorithms in federated learning. *arXiv preprint arXiv:2008.03606*, 2020a.
- S. P. Karimireddy, S. Kale, M. Mohri, S. Reddi, S. Stich, and A. T. Suresh. Scaffold: Stochastic controlled averaging for federated learning. In *ICML*, pages 5132–5143. PMLR, 2020b.
- D. Kermany, K. Zhang, M. Goldbaum, et al. Labeled optical coherence tomography (oct) and chest x-ray images for classification. *Mendeley data*, 2(2):651, 2018.
- G. Kim, J. Kim, and B. Han. Communication-efficient federated learning with accelerated client gradient. In *Proceedings of the IEEE/CVF CVPR*, pages 12385–12394, 2024.
- A. Krizhevsky, G. Hinton, et al. Learning multiple layers of features from tiny images. 2009.

- J. N. Kundu, A. Kulkarni, A. Singh, V. Jampani, and R. V. Babu. Generalize then adapt: Source-free domain adaptive semantic segmentation. In *Proceedings of the IEEE/CVF ICCV*, pages 7046–7056, 2021.
- D. Li and J. Wang. Fedmd: Heterogenous federated learning via model distillation. *arXiv preprint arXiv:1910.03581*, 2019.
- H. Li, Z. Cai, J. Wang, J. Tang, W. Ding, C.-T. Lin, and Y. Shi. Fedtp: Federated learning by transformer personalization. *IEEE transactions on neural networks and learning systems*, 2023a.
- T. Li, A. K. Sahu, M. Zaheer, M. Sanjabi, A. Talwalkar, and V. Smith. Federated optimization in heterogeneous networks. *Proceedings of Machine learning and systems*, 2:429–450, 2020.
- T. Li, S. Hu, A. Beirami, and V. Smith. Ditto: Fair and robust federated learning through personalization. In *ICML*. PMLR, 2021a.
- X. Li, M. Jiang, X. Zhang, M. Kamp, and Q. Dou. Fedbn: Federated learning on non-iid features via local batch normalization. *arXiv preprint arXiv:2102.07623*, 2021b.
- Y. Li, N. Wang, J. Shi, and X. Hou. Revisiting batch normalization for practical domain adaptation. *arXiv preprint arXiv:1603.04779*, 2016.
- Z. Li, Q. Li, Y. Zhou, W. Zhong, G. Zhang, and C. Wu. Edge-cloud collaborative learning with federated and centralized features. In *Proceedings of the 46th International ACM SIGIR Conference on Research and Development in IR*, pages 1949–1953, 2023b.
- Z. Li, T. Lin, X. Shang, and C. Wu. Revisiting weighted aggregation in federated learning with neural networks. In *ICML*. PMLR, 2023c.
- Q. Lian, F. Lv, L. Duan, and B. Gong. Constructing self-motivated pyramid curriculums for cross-domain semantic segmentation: A non-adversarial approach. In *Proceedings of the IEEE/CVF ICCV*, 2019.
- P. P. Liang, T. Liu, L. Ziyin, N. B. Allen, R. P. Auerbach, D. Brent, R. Salakhutdinov, and L.-P. Morency. Think locally, act globally: Federated learning with local and global representations. *arXiv preprint arXiv:2001.01523*, 2020.
- B. Liu, Y. Guo, and X. Chen. Pfa: Privacy-preserving federated adaptation for effective model personalization. In *Proceedings of the Web Conference 2021*, pages 923–934, 2021a.
- Y. Liu, W. Zhang, and J. Wang. Source-free domain adaptation for semantic segmentation. In *Proceedings of the IEEE/CVF CVPR*, 2021b.
- M. Long, Y. Cao, J. Wang, and M. Jordan. Learning transferable features with deep adaptation networks. In *ICML*. PMLR, 2015.
- Y. Luo, L. Zheng, T. Guan, J. Yu, and Y. Yang. Taking a closer look at domain shift: Category-level adversaries for semantics consistent domain adaptation. In *Proceedings of the IEEE/CVF CVPR*, 2019.

- X. Ma, J. Zhang, S. Guo, and W. Xu. Layer-wised model aggregation for personalized federated learning. In *Proceedings of the IEEE/CVF CVPR*, pages 10092–10101, 2022.
- Y. Mansour, M. Mohri, J. Ro, and A. T. Suresh. Three approaches for personalization with applications to federated learning. *arXiv preprint arXiv:2002.10619*, 2020.
- O. Marfoq, G. Neglia, R. Vidal, and L. Kameni. Personalized federated learning through local memorization. In *ICML*. PMLR, 2022.
- F. Maria Carlucci, L. Porzi, B. Caputo, E. Ricci, and S. Rota Bulò. Autodial: Automatic domain alignment layers. In *Proceedings of the IEEE ICCV*, pages 5067–5075, 2017.
- McMahan et al. Communication-efficient learning of deep networks from decentralized data. In *AIS*, pages 1273–1282. PMLR, 2017.
- M. Mendieta, T. Yang, P. Wang, M. Lee, Z. Ding, and C. Chen. Local learning matters: Rethinking data heterogeneity in federated learning. In *Proceedings of the IEEE/CVF CVPR*, pages 8397–8406, 2022.
- J. Nguyen, J. Wang, K. Malik, M. Sanjabi, and M. Rabbat. Where to begin? on the impact of pre-training and initialization in federated learning. *arXiv preprint arXiv:2206.15387*, 2022.
- X. Peng, Z. Huang, Y. Zhu, and K. Saenko. Federated adversarial domain adaptation. *arXiv preprint arXiv:1911.02054*, 2019.
- L. Qu, Y. Zhou, P. P. Liang, Y. Xia, F. Wang, E. Adeli, L. Fei-Fei, and D. Rubin. Rethinking architecture design for tackling data heterogeneity in federated learning. In *Proceedings of the IEEE/CVF CVPR*, pages 10061–10071, 2022.
- P. Ramachandran, N. Parmar, A. Vaswani, I. Bello, A. Levskaya, and J. Shlens. Stand-alone self-attention in vision models. *Advances in NeurIPS*, 32, 2019.
- S. R. Richter, V. Vineet, S. Roth, and V. Koltun. Playing for data: Ground truth from computer games. In *Computer Vision–ECCV 2016: 14th European Conference, Amsterdam, The Netherlands, October 11–14, 2016, Proceedings, Part II 14*, pages 102–118. Springer, 2016.
- K. Saenko, B. Kulis, M. Fritz, and T. Darrell. Adapting visual category models to new domains. In *Computer Vision–ECCV 2010: 11th ECCV Proceedings, Part IV 11*. Springer, 2010.
- K. Saito, K. Watanabe, Y. Ushiku, and T. Harada. Maximum classifier discrepancy for unsupervised domain adaptation. In *Proceedings of the IEEE CVPR*, pages 3723–3732, 2018.
- F. Sattler, S. Wiedemann, K.-R. Müller, and W. Samek. Robust and communication-efficient federated learning from non-iid data. *IEEE transactions on neural networks and learning systems*, 31(9):3400–3413, 2019.

- F. Sattler, K.-R. Müller, and W. Samek. Clustered federated learning: Model-agnostic distributed multitask optimization under privacy constraints. *IEEE transactions on neural networks and learning systems*, 32(8):3710–3722, 2020.
- W. Shakespeare. The complete works of william shakespeare. <http://www.gutenberg.org/files/100/old/1994-01-100.zip>, 1994. Accessed on 21-03, 2024.
- G. Sun, M. Mendieta, J. Luo, S. Wu, and C. Chen. Fedperfix: Towards partial model personalization of vision transformers in federated learning. In *Proceedings of the IEEE/CVF ICCV*, pages 4988–4998, 2023.
- C. T Dinh, N. Tran, and J. Nguyen. Personalized federated learning with moreau envelopes. *Advances in NeurIPS*, 33, 2020.
- Tan et al. Towards personalized federated learning. *IEEE Transactions on NNLS*, 2022.
- P. Testolina, F. Barbato, U. Michieli, M. Giordani, P. Zanuttigh, and M. Zorzi. Selma: Semantic large-scale multimodal acquisitions in variable weather, daytime and viewpoints. *IEEE Transactions on Intelligent Transportation Systems*, 2023.
- M. Toldo, A. Maracani, U. Michieli, and P. Zanuttigh. Unsupervised domain adaptation in semantic segmentation: a review. *Technologies*, 8(2):35, 2020.
- N. H. Tran, W. Bao, A. Zomaya, M. N. Nguyen, and C. S. Hong. Federated learning over wireless networks: Optimization model design and analysis. In *IEEE INFOCOM 2019-IEEE conference on computer communications*, pages 1387–1395. IEEE, 2019.
- Y.-H. Tsai, W.-C. Hung, S. Schuler, K. Sohn, M.-H. Yang, and M. Chandraker. Learning to adapt structured output space for semantic segmentation. In *Proceedings of the IEEE CVPR*, pages 7472–7481, 2018.
- F. Varno, M. Saghai, L. Rafiee Severyi, S. Gupta, S. Matwin, and M. Havaei. Adabest: Minimizing client drift in federated learning via adaptive bias estimation. In *European Conference on Computer Vision*, pages 710–726. Springer, 2022.
- A. Vaswani, N. Shazeer, N. Parmar, J. Uszkoreit, L. Jones, A. N. Gomez, L. Kaiser, and I. Polosukhin. Attention is all you need. *Advances in NeurIPS*, 30, 2017.
- K. Wang, R. Mathews, C. Kiddon, H. Eichner, F. Beaufays, and D. Ramage. Federated evaluation of on-device personalization. *arXiv preprint arXiv:1910.10252*, 2019.
- W. Wang, J. Dai, Z. Chen, Z. Huang, Z. Li, X. Zhu, X. Hu, T. Lu, L. Lu, H. Li, et al. Internimage: Exploring large-scale vision foundation models with deformable convolutions. In *Proceedings of the IEEE/CVF CVPR*, pages 14408–14419, 2023.
- X. Wang, Y. Peng, L. Lu, Z. Lu, M. Bagheri, and R. M. Summers. Chestx-ray8: Hospital-scale chest x-ray database and benchmarks on weakly-supervised classification and localization of common thorax diseases. In *Proceedings of the IEEE CVPR*, pages 2097–2106, 2017.

- J. Xu, S. Wang, L. Wang, and A. C.-C. Yao. Fedcm: Federated learning with client-level momentum. *arXiv preprint arXiv:2106.10874*, 2021.
- J. Yang, C. Li, X. Dai, and J. Gao. Focal modulation networks. *Advances in NeurIPS*, 35: 4203–4217, 2022.
- Y. Yang and S. Soatto. Fda: Fourier domain adaptation for semantic segmentation. In *Proceedings of the IEEE/CVF CVPR*, 2020.
- C.-H. Yao, B. Gong, H. Qi, Y. Cui, Y. Zhu, and M.-H. Yang. Federated multi-target domain adaptation. In *Proceedings of the IEEE/CVF WACV*, pages 1424–1433, 2022.
- J. Zhang, S. Guo, Z. Qu, D. Zeng, Y. Zhan, Q. Liu, and R. Akerkar. Adaptive federated learning on non-iid data with resource constraint. *IEEE Transactions on Computers*, 71(7):1655–1667, 2021a.
- J. Zhang, Z. Qu, C. Chen, H. Wang, Y. Zhan, B. Ye, and S. Guo. Edge learning: The enabling technology for distributed big data analytics in the edge. *ACM Computing Surveys*, 54(7):1–36, 2021b.
- J. Zhang, Y. Hua, H. Wang, T. Song, Z. Xue, R. Ma, and H. Guan. Fedala: Adaptive local aggregation for personalized federated learning. In *Proceedings of the AAAI Conference on Artificial Intelligence*, volume 37, pages 11237–11244, 2023a.
- J. Zhang, Y. Hua, H. Wang, T. Song, Z. Xue, R. Ma, and H. Guan. Fedcp: Separating feature information for personalized federated learning via conditional policy. In *Proceedings of the 29th ACM SIGKDD Conference on KD and Data Mining*, pages 3249–3261, 2023b.
- L. Zhang, Y. Shi, Y.-C. Chang, and C.-T. Lin. Federated fuzzy neural network with evolutionary rule learning. *IEEE Transactions on Fuzzy Systems*, 2022a.
- W. Zhang, X. Chen, L. Xu, X. Wang, and S. Yang. Semi-asynchronous personalized federated learning for short-term photovoltaic power forecasting. *Digital Communications and Networks*, 2022b.
- W. Zhang, F. Yu, X. Wang, F.-Y. Zeng, L. Li, and Z. Li. Resilient reinforcement federated learning for industrial applications. *IEEE Transactions on Industrial Informatics*, 2022c.
- Y. Zhao, M. Li, L. Lai, N. Suda, D. Civin, and V. Chandra. Federated learning with non-iid data. *arXiv preprint arXiv:1806.00582*, 2018.
- Z. Zhu, J. Hong, and J. Zhou. Data-free knowledge distillation for heterogeneous federated learning. In *ICML*. PMLR, 2021.
- X. Zou, Z.-Y. Dou, J. Yang, Z. Gan, L. Li, C. Li, X. Dai, H. Behl, J. Wang, L. Yuan, et al. Generalized decoding for pixel, image, and language. In *Proceedings of the IEEE/CVF CVPR*, 2023.
- Y. Zou, Z. Yu, B. Kumar, and J. Wang. Unsupervised domain adaptation for semantic segmentation via class-balanced self-training. In *Proceedings of the ECCV*, pages 289–305, 2018.